Electronic Supplementary Material (ESI) for Catalysis Science & Technology.
This journal is © The Royal Society of Chemistry 2020

The Role of the Surface Properties in CO_2 Methanation over Carbon-Supported Ni Catalysts and their Promotion by Fe

Liliana P. L. Gonçalves,[a, b] Juliana P. S. Sousa,[a] O. Salomé G. P. Soares,[b] Oleksandr Bondarchuk,[a] Oleg I. Lebedev,[c] Yury V. Kolen'ko,[a,*] M. Fernando R. Pereira,[b,*]

[a] International Iberian Nanotechnology Laboratory (INL), Avenida Mestre José Veiga, 4715-330 Braga, Portugal

[b] Laboratory of Separation and Reaction Engineering – Laboratory of Catalysis and Materials (LSRE-LCM), Faculdade de Engenharia, Universidade do Porto, Rua Dr. Roberto Frias, 4200-465 Porto, Portugal

[c] Laboratoire CRISMAT, UMR 6508, CNRS-ENSICAEN, Caen 14050, France

Experimental

Materials

Activated carbon (**AC**) NORIT GAC 1240 PLUS was obtained from CABOT, $Ni(NO_3)_2{\cdot}6H_2O$ (≥ 97.0%) and $Fe(NO_3)_3{\cdot}6H_2O$ (≥ 98.0%) were purchased from Sigma Aldrich and Melamine (≥ 99%) from Fluka.

Preparation of the supporting materials with different surface functionalities

Three different treatments were performed on a commercial AC (Norit GAC 1240Plus) in other to obtain materials with different surface chemistries.

In order to prepare oxidized AC (AC–O), 7 g of AC was placed in a 100 mL extraction Soxhlet. In attached 250 mL round bottom flask, 5 M HNO_3 was heated until its boiling point and the system was maintained under reflux for 6 h. After that, the material was washed with distilled water until neutral pH and finally dried at 120 °C.[24]

To prepare N-doped AC (AC–N), 1.8 g of AC and 1.17 g of melamine were ball milled in a closed pot for 2 h at a vibration frequency of 15 vibrations s^{-1} using a Retsch MM200 ball-milling equipment. After that, the mixture was annealed at 600 °C for 1 h under 100 $cm^3\ min^{-1}$ flow of N_2.[40]

To obtain an oxygen-free surface with Lewis base sites (AC–R), 3 g of AC was placed in a quartz tube reactor and heated to 900 °C at 10 °C min^{-1} under a N_2 flow of 100 $cm^3\ min^{-1}$. When 900 °C was reached, the flow was changed to 50 $cm^3\ min^{-1}$ of H_2 and the system was maintained at 900 °C for 1 h.[41]

Preparation of the Ni and NiFe catalysts

Carbon-supported Ni nanocatalysts were prepared by incipient wetness impregnation (IWI) method. 0.5 g of the respective supporting material was placed under ultrasonic vibration and an aqueous solution of $Ni(NO_3)_2{\cdot}6H_2O$ was added to obtain a Ni loading of 15 wt%. The sample was left under ultrasonic vibration for other 90 min, and after that was dried at 120 °C overnight. The loading was selected by preliminary screening of the catalysts with different loadings of Ni (5 %, 15 %, and 25 %) on **AC** in CO_2 methanation, and an optimal Ni loading was established to be 15 wt%.

The NiFe catalysts were prepared similarly, by sequential impregnation. 0.5 g of **AC–R** supporting material was placed under ultrasonic vibration and an aqueous solution of $Ni(NO_3)_2{\cdot}6H_2O$ was added first to obtain a Ni loading of 15 wt%. The sample was left under ultrasonic vibration for other 90 min and after that was dried at 120 °C overnight. Next, the Ni-containing sample was placed under ultrasonic vibration again and an aqueous solution of $Fe(NO_3)_2{\cdot}9H_2O$ was added to obtain a Fe loading of 5 wt%. The loading and Ni:Fe ratio were selected by preliminary methanation tests, where firstly, different Ni-Fe ratios were tested and 3:1 was found to be optimal, and then the total loading was varied while preserving Ni:Fe ration of 3:1, and total metal loading of 20 wt% was established to be an optimal one.

Finally, all samples are annealed under N_2 and reduced under H_2 at the respective temperature determined by H_2 temperature programmed reduction (H_2–TPR). The samples were placed in a quartz tube reactor and heated to the desired temperature at 10 °C min^{-1} under a N_2 flow of 100 $cm^3\ min^{-1}$ and annealed for 1 h. After that, the flow was switched to 50 $cm^3\ min^{-1}$ of H_2 and the sample was reduced during 3 h.

Characterization

The N_2 adsorption-desorption isotherms at −196 °C were collected using a Quantachrome NOVA 4200e multi-station apparatus. Previous to the physisorption analysis, the samples (c.a. 100 mg) were degassed at 170 °C for 3 h. The surface area (S_{BET}) was calculated by the Brunauer-Emmett-Teller (BET) method, the mesopore surface area (S_{meso}) and the micropore volumes (V_{micro}) were calculated by the t-method, and the total specific pore volume (V_p) was determined from the amount of N_2 adsorbed at relative pressure $P/P_0 = 0.95$.

Elemental analysis was carried out on a vario MICRO cube analyser from Elemental GmbH in CHNS mode. Each element (CHNS) was determined by combustion of the sample at 1050 °C and calculated by the mean of three independent measurements, using a per-day calibration with a standard compound. Ash content was determined by thermogravimetric analysis (TGA) using a Mettler-Toledo TGA/DSC 1 STAR equipment, by heating the samples under Ar flow from 50 to 900 °C, at a heating rate of 10 °C min^{-1}, while performing two isothermal steps: 7 min under Ar and 13 min under air. The O content was determined by difference.

The point of zero charge (pH_{PZC}) was determined by placing 20 mg of the sample in closed Erlenmeyer flasks with 20 mL of 0.01 M NaCl solution, to which the pH was adjusted to a value between 2 and 12 by adding either 0.1 M HCl or 0.1 M NaOH solutions. The Erlenmeyer flasks with different pH were left for 24 h under stirring at room temperature. The final pH was measured for each sample, as well as for a blank experiment (without material, $pH_{initial}$). The pH_{PZC} is the point where the curve pH_{final} versus $pH_{initial}$ crosses the line $pH_{initial}=pH_{final}$.

X-ray photoelectron spectroscopy (XPS) measurements were performed using a monochromated microfocused Al Kα X-ray source. Powdered samples were pressed into carbon tape, which was directly attached to the sample holder. Charge neutralization was provided by a flood gun producing low-energy (≤ 1 eV) beams of Ar^+ ions and electrons. Fitting of the XPS spectra was performed using the Avantage software from Thermo Fisher Scientific, in which the peaks were fitted with a Gaussian–Lorentzian function. Binding energies were calibrated relative to the C 1s peak for aliphatic and aromatic carbon at 284.6 eV.

Transmission electron microscopy (TEM) studies were conducted using a JEOL 2100 microscope operated at 200 kV. Additionally, TEM, high-angle annular dark-field scanning transmission electron microscopy (HAADF-STEM), electron diffraction (ED), and energy-dispersive X-ray spectroscopy in STEM mode (STEM–EDX) were performed using JEM-ARM200F cold FEG probe and image aberration corrected microscope, operated at 200 kV and equipped with large angle CENTURIO EDX detector and QUANTUM GIF. The samples were dispersed in ethanol and placed onto a copper grid. The particle size distribution was obtained by measuring at least 200 particles using ImageJ software.

Powder X-ray diffraction (XRD) analysis was performed using a PANanalytical X'Pert PRO diffractometer with Ni filtered Cu K_α radiation and a PIXcel detector. The sample is grounded to a fine powder and placed in the sample holder. A Bragg Brentano configuration was used in a 2θ range from 20° to 80° with step size of 0.01° and a time per step of 300 s. Collected data was analyzed using PANanalytical High Score software.

H_2 temperature programmed reduction (H_2–TPR) analysis was performed using an AMI–200 Catalyst Characterization apparatus from Altamira Instruments, equipped with a thermal conductivity detector (TCD), high precision mass flow controllers and adjustable furnace with air cooling. Approximately 100 mg of sample was placed in a U-shaped quartz tube in a furnace. Before the heating phase, Ar (25 cm^3 min^{-1}) was used to flush the tube, and then H_2 diluted in Ar (5% H_2/Ar) was used as reducing atmosphere. While the reducing gas was going through the tube, the temperature was raised until 1000 °C with a heating rate of 10 °C min^{-1}.

H_2 pulse chemisorption analysis was performed using an AMI–200 Catalyst Characterization apparatus from Altamira Instruments, equipped with a thermal conductivity detector (TCD), high precision mass flow controllers and adjustable furnace with air cooling. Approximately 100 mg of sample was placed in a U-shaped quartz tube in a furnace. The sample was pre-treated *in situ* under H_2 for 30 min at the reduction temperature, cooled down to 40 °C and flushed with Ar. After that, pulses of 58 μL of H_2 were injected in the carrier gas (Ar, 25 cm^3 min^{-1}) until the area of the hydrogen peak on the chromatograph was identical. The Ni surface area was calculated by assuming the adsorption stoichiometry of one hydrogen atom per nickel surface atom.

Temperature Programmed Desorption (TPD) analysis was performed using an AMI–300 Catalyst Characterization apparatus from Altamira Instruments, equipped with a thermal conductivity detector (TCD) and a Mass Spectrometer (MS), high precision mass flow controllers and adjustable furnace with air cooling. Approximately 100 mg of catalyst was placed in a U-shaped quartz tube in a furnace. The sample was pre-treated *in situ* under H_2 for 30 min at the reduction temperature and cooled down to 40 °C under He. After that, the temperature was increase until 1050 °C under He (25 cm^3 min^{-1}). The amount of CO and CO_2 released by the sample was analysed by MS.

CO_2 Methanation Catalytic Experiments

The catalytic experiments were carried out in a Microactivity XS15 system from PID Eng & Tech, using a fixed bed quartz reactor ($d_{int} = 1$ cm), and the products in the outflow were analyzed online by a gas chromatograph (GC 1000 from DANI) equipped with a thermal conductivity detector (TCD) and a GS-CarbonPLOT capillary column, with He as carrier gas, using a continuous flow of N_2 as internal standard. A condenser in the Microactivity XS15 system condensates the water formed before the gas was injected in the GC. The catalyst (100 mg) was mixed with inert SiC (to assure a significant bed height and a good space velocity) and placed in a fixed bed quartz reactor. Each catalyst was pre-treated *in situ* under H_2 flow (40 cm^3 min^{-1}) at the reduction temperature for 30 min, at 1 bar. After that, the reactor temperature was decreased to 200 °C under He (50 cm^3 min^{-1}), and then, the reactor was fed with 10% CO_2, 40% H_2 (the stoichiometric composition) and 50% He. A temperature ramping from 200 °C to 500 °C was performed under reaction conditions in order to evaluate the performance of each sample at various temperatures.

To evaluate the stability of the best performing sample, the experiment was performed under the same conditions referred before; however, under isothermal conditions at the established optimal temperature.

Conversion of CO_2 (X_{CO2}), selectivity to methane (S_{CH4}) and CO (S_{CO}), and yield to methane (Y_{CH4}) were calculated as following, considering CO as the only by-product:

$$\mathrm{X}\ (\%) = \frac{[CO_2]_{in} - [CO_2]_{out}}{[CO_2]_{in}} \times 100 \tag{1}$$

$$S_{\mathrm{CH_4}} = \frac{[CH_4]_{out}}{[CH_4]_{out} + [CO]_{out}} \times 100 \tag{2}$$

$$S_{CO} = \frac{[CO]_{out}}{[CH_4]_{out} + [CO]_{out}} \times 100 \tag{3}$$

$$Y_{\mathrm{CH_4}} = \frac{X \times S_{\mathrm{CH_4}}}{100} \tag{4}$$

Where $[CO_2]_{in}$ and $[CO_2]_{out}$ are the concentration of CO_2 in moles min^{-1} in the inlet and outlet flow, respectively. $[CH_4]_{out}$ is the concentration of CH_4 in moles min^{-1} in the outlet flow, and $[CO]_{out}$ is the concentration of CO in moles min^{-1} in the outlet flow.

Simulation of Thermodynamic Equilibrium of CO_2 Methanation

Thermodynamic equilibrium analysis was performed by the simulation software HSC Chemistry®. The equilibrium compositions of the system were determined at specified operating conditions (temperature, pressure and feed composition) using a model based on the minimization of Gibbs free-energy of the existing species (CH_4, H_2O, CO_2, CO, H_2, solid carbon).

Characterization of Supporting carbon materials

N_2 physisorption

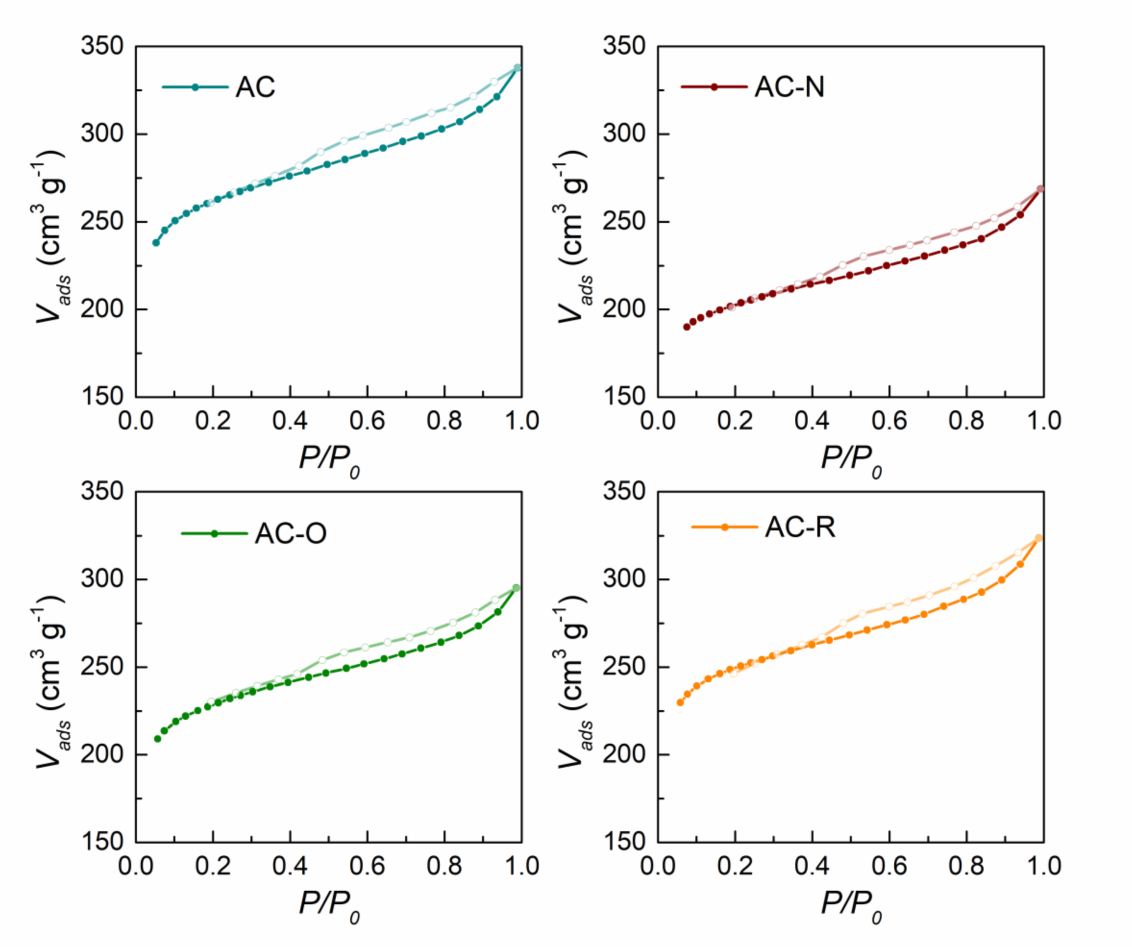

Fig. S1 Comparison of N_2 adsorption–desorption isotherms measured at –196 °C for the pristine **AC**, N-doped **AC–N**, oxidized **AC–O** and reduced **AC–R** supporting materials.

Table S1. Elemental composition and textural properties of pristine AC and as-synthesized AC–N, AC–O and AC–R.

SAMPLE	N (%)	C (%)	H (%)	S (%)	O (%)	S_{BET} (M^2 G^{-1})	$V_{P,P/P0=0.95}$ (CM^3 G^{-1})	V_{MICRO} (CM^3 G^{-1})
AC	0.0	85.4	2.1	0.4	7.0	784	0.50	0.34
AC–N	5.8	79.7	2.4	0.1	6.9	622	0.39	0.26
AC–O	0.2	82.7	2.4	0.2	9.5	720	0.44	0.30
AC–R	0.0	88.5	2.1	0.0	3.8	768	0.48	0.33

X-ray photoelectron spectroscopy

Five peaks were identified in the C 1s region (Fig. S2, left), which correspond to the aromatic and aliphatic carbon, as well as C–NH$_2$ (C$_{ar,al}$,C–NH$_2$) at 284.6 eV, the hydroxyl groups and C–N (COH, CN) at 286.0 ± 0.2 eV, carbonyl groups (C=O) at 287.8 ± 0.2 eV, carboxylic groups (COOH) at 289.5 ± 0.2 eV, and the plasmon loss (C$_{shake-up}$) at 291.2 ± 0.2 eV.[49]

Regarding O 1s region (Fig. S2, right), five peaks were identified, which correspond to oxygen in C=O groups (O1) at 531.3 ± 0.1 eV; hydroxyls, ethers and C=O in esters, amides, anhydrides (O2) at 532.2 ± 0.1 eV, C–O groups in esters and anhydrides (O3) at 533.4 ± 0.1 eV; carboxylic groups (O4) at 534.5 ± 0.1 eV, and water at 536.3 ± 0.1 eV. Furthermore, the N content is null in all samples, except **AC–N**, which presents majorly pyridinic groups (N-6) at 398.3 eV, but also pyrrolic (N-5) at 400.0 eV, quaternary (N-Q) at 401.4 eV and also nitrogen–oxygen complexes (NX) at 403.4 eV (Fig. S3).[49]

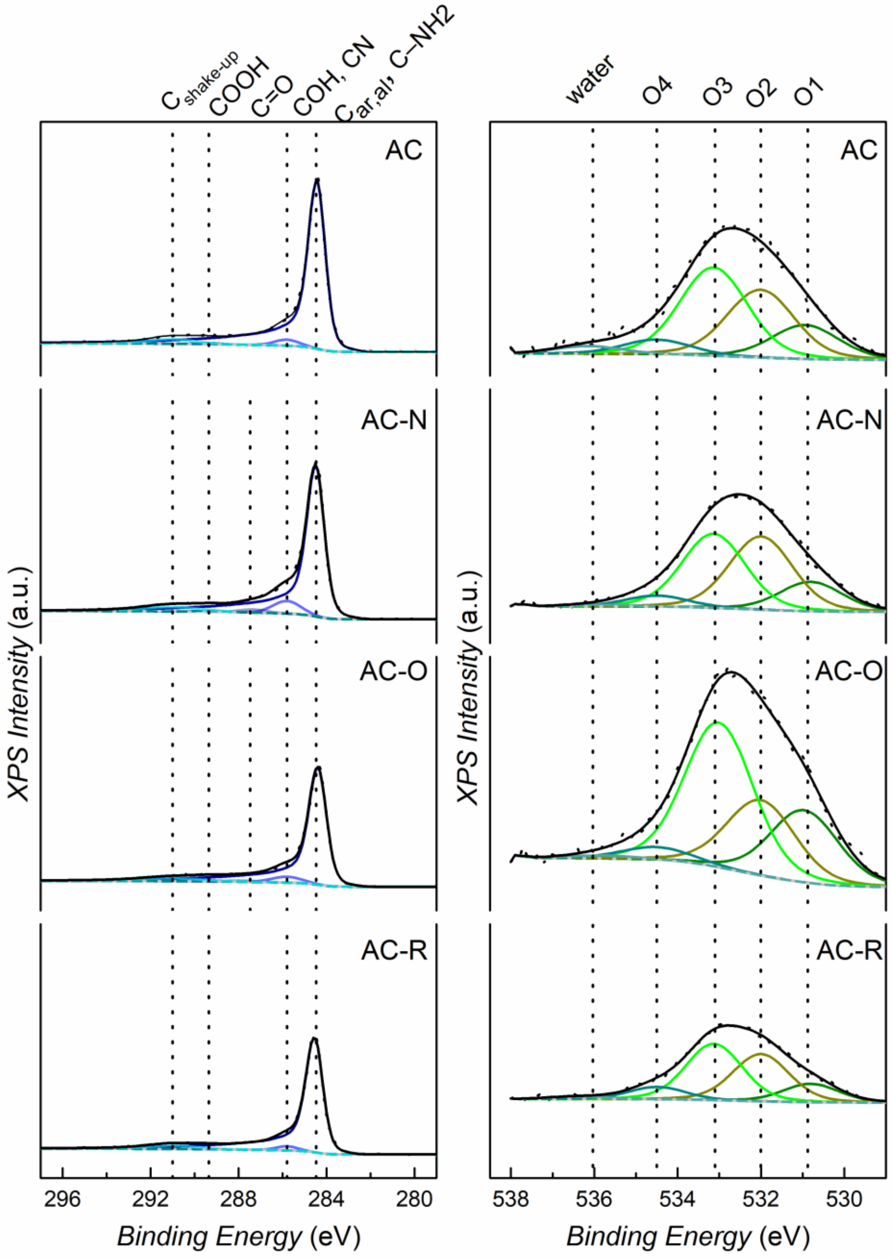

Fig. S2 High-resolution XPS data for C 1s region (left) and O 1s region (right) for pristine **AC**, N-doped **AC–N**, oxidized **AC–O** and reduced **AC–R** supporting materials. Symbols: raw data; black lines: overall fits; colored lines: fits of individual components; dashed lines: background. C$_{ar,al}$, C–NH$_2$: aromatic and aliphatic carbon; COH, CN: hydroxyl groups, CN; C=O: carbonyl groups; COOH: carboxylic groups; C$_{shake-up}$: plasmon loss. O1: C=O; O2: hydroxyls, ethers and C=O in esters, amides, anhydrides; O3: C–O in esters and anhydrides; O4: carboxylic groups.

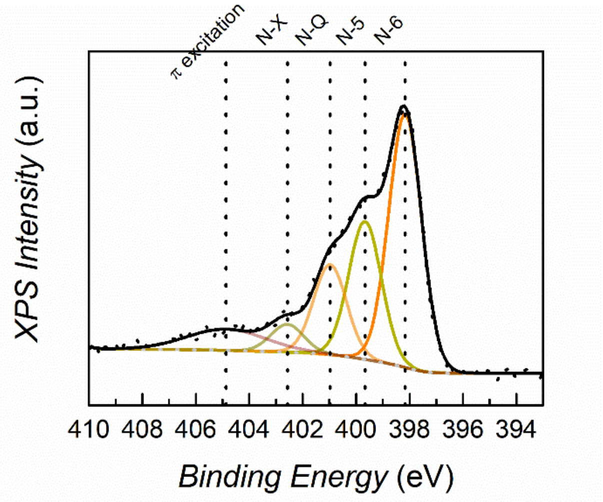

Fig. S3 High-resolution XPS data for N 1s region for **AC–N**. Symbols: raw data; black lines: overall fits; colored lines: fits of individual components; dashed lines: background. N-6: Pyridinic groups; N-5: Pyridonic or pyrrolic groups; N-Q: Quaternary groups; N-X: Nitrogen oxides or nitrates.

Table S2. Surface elemental composition of pristine AC and synthesized AC–N, AC–O, and AC–R supporting materials, determined by XPS.

SAMPLE	*N_{XPS} (at%)*	*C_{XPS} (at%)*	*O_{XPS} (at%)*	*Total oxygen to total carbon O_t/C_t*
AC	0	95.7	4.3	0.045
AC–N	8.1	88.6	3.4	0.038
AC–O	1.3	90.6	8.1	0.089
AC–R	0	96.6	3.4	0.035

Characterization of the as-synthesized Catalysts

N_2 physisorption

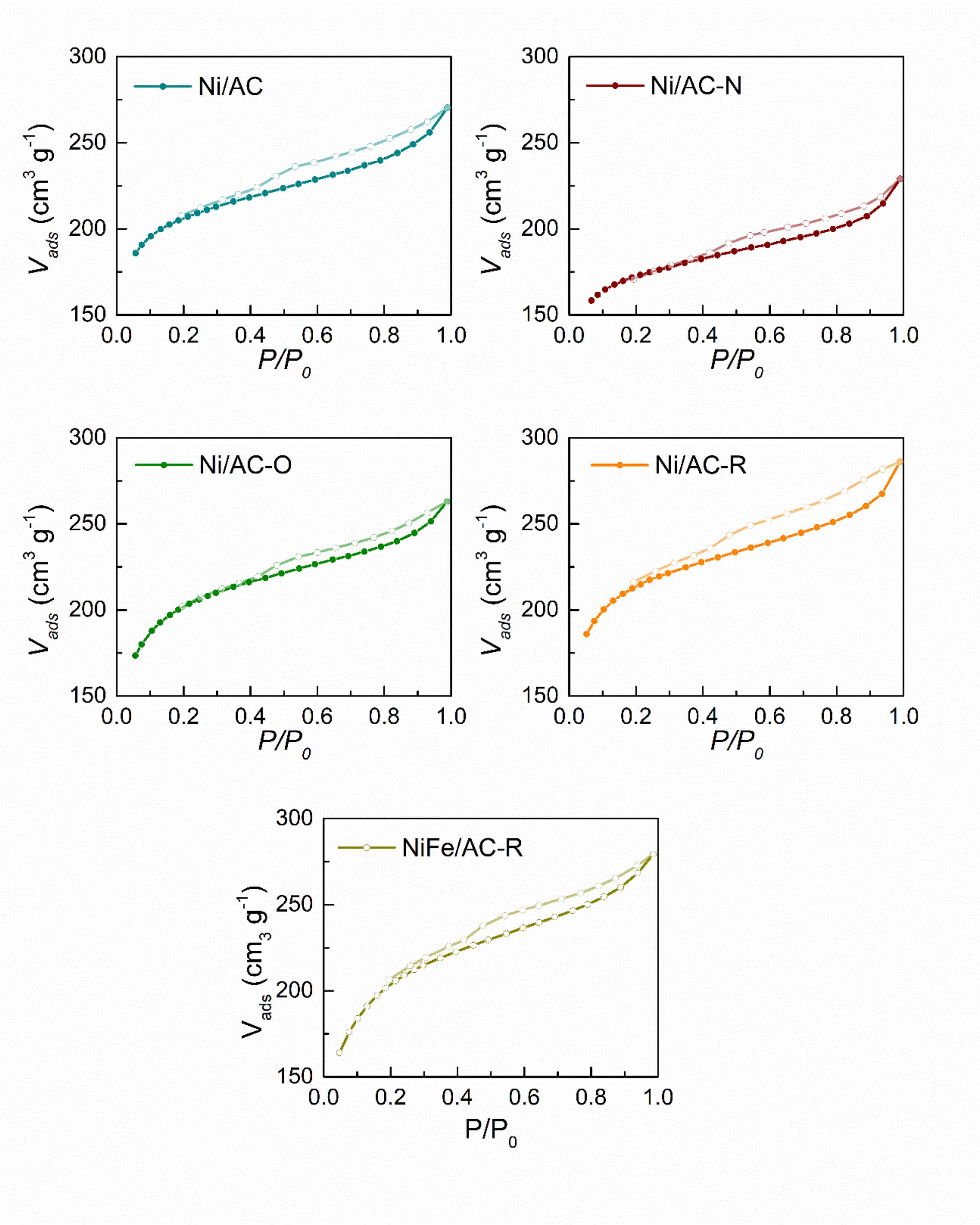

Fig. S4 Comparison of N_2 adsorption–desorption isotherms measured at −196 °C for the as-synthesized CO_2 methanation catalysts **Ni/AC**, **Ni/AC–N**, **Ni/AC–O**, **Ni/AC–R**, and **NiFe/AC–R**.

Transmission electron microscopy

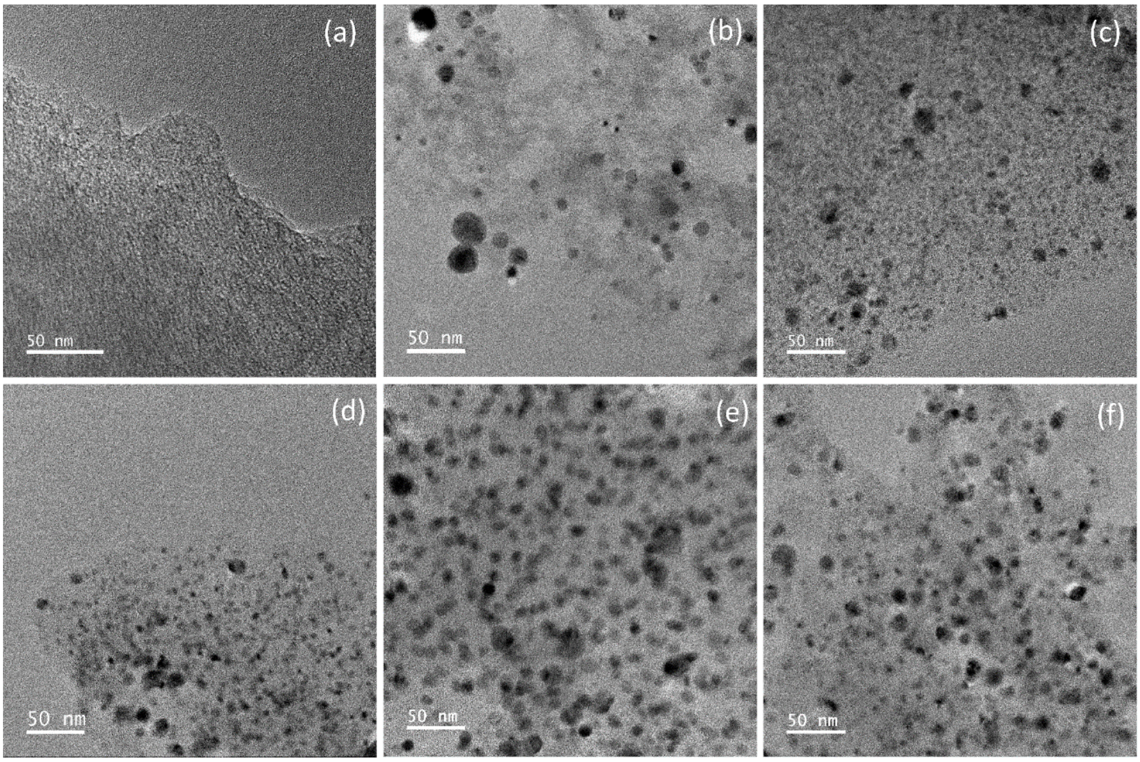

Fig. S5 Low-magnification TEM images of **AC** (a) **Ni/AC** (b), **Ni/AC–N** (c), **Ni/AC–O** (d), **Ni/AC–R** (e), and bimetallic **NiFe/AC–R** catalysts for CO_2 methanation.

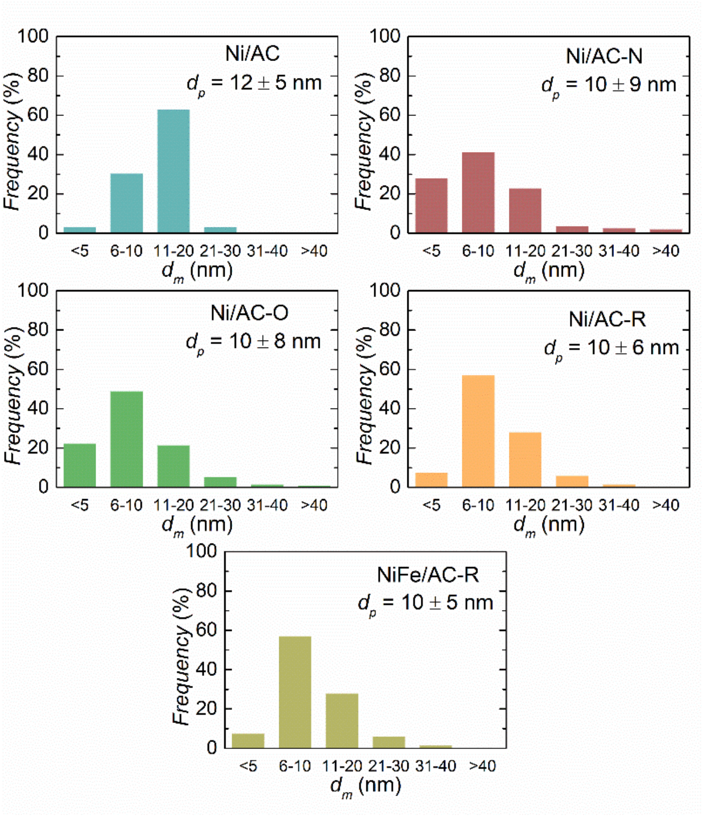

Fig. S6 Comparison of the size distribution of Ni NPs in **Ni/AC**, **Ni/AC–N**, **Ni/AC–O**, **Ni/AC–R**, and bimetallic **NiFe/AC–R**, estimated from TEM images.

Temperature Programmed Desorption (TPD)

Three peaks were identified in the deconvolution of the CO evolution in the TPD analysis of the samples (Fig. S7) and they correspond to (1) carboxylic anhydrides, (2) phenols, and (3) carbonyl/quinones. It is important to note that N_2 presents the same m/z than CO, thus, in the case of sample **Ni/AC–N**, the amount of CO is higher due to contribution of N_2. Regarding CO_2 evolution profile, all samples present a first sharp peak below 400 °C, even though the sample was pre-treated at this temperature, which is characteristic of a catalytic decomposition of the material promoted by Ni,[43] followed by a peak above 400 °C, corresponding to the oxygen functional groups present in the material.

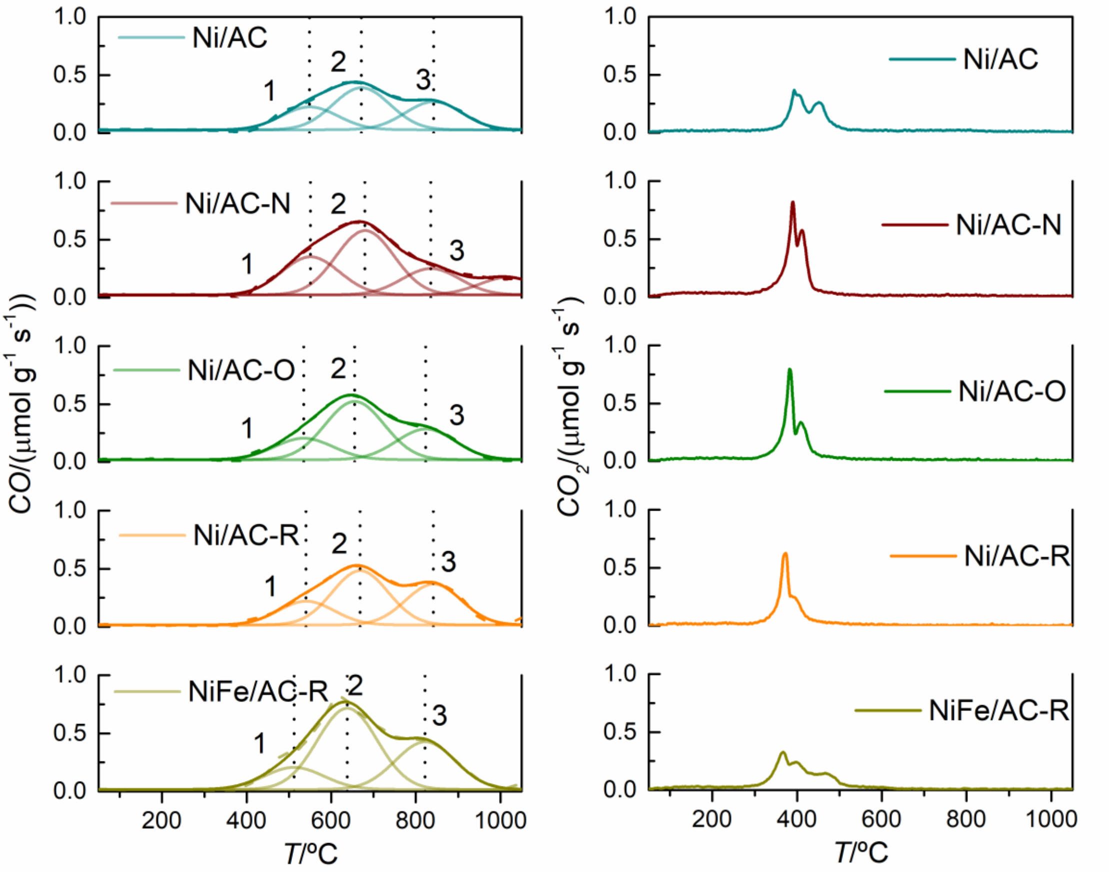

Fig. S7 TPD profiles of **Ni/AC**, **Ni/AC–N**, **Ni/AC–O**, **Ni/AC–R**, and bimetallic **NiFe/AC–R**, showing the CO (left) and CO_2 (right) evolution. The CO evolution peak was deconvoluted in three peaks: (1) carboxylic anhydrides; (2) phenols; (3) carbonyl/quinones.

Table S3. Relative percentage of each peak, corresponding to the different groups ((1) carboxylic anhydrides, (2) phenols, and (3) carbonyl/quinones) in the CO evolution graphic.

SAMPLE	*CO Peak 1 (%)*	*CO Peak 2 (%)*	*CO Peak 3 (%)*
Ni/AC	25	45	30
Ni/AC–N	30	50	20
Ni/AC–O	19	53	28
Ni/AC–R	20	46	34
NiFe/AC–R	15	54	32

Simulation of Thermodynamic Equilibrium of CO_2 Methanation

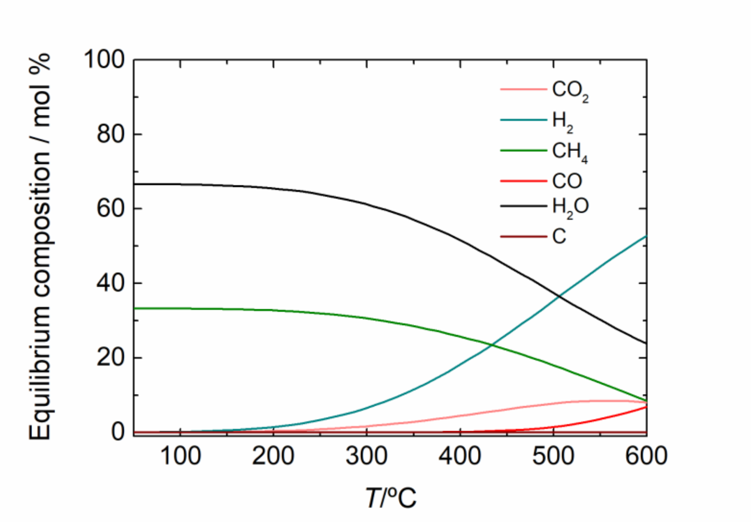

Figure S8. Thermodynamic equilibrium composition as a function of the temperature.

Catalysts Characterization after prolonged catalytic testing

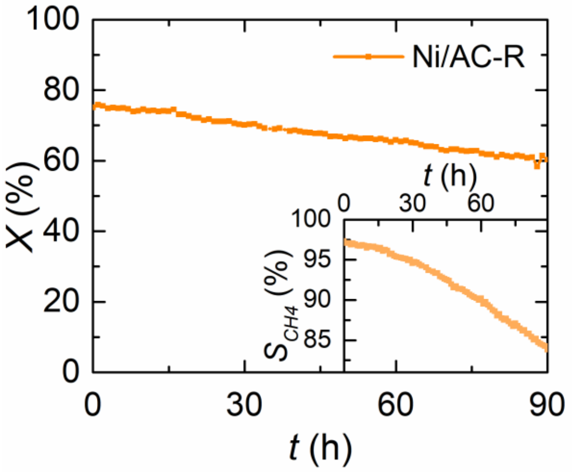

Fig. S9 X_{CO2} and S_{CH4} as a function of a prolonged time on stream (90 h) at 450 °C for **Ni/AC-R**. Reaction conditions: *P* = 1 bar; *WHSV* = 60 000 mL g^{-1} h^{-1}; $CO_2 : H_2 = 1 : 4$.

Characterization of the Ni/AC–R before and afterTOS

Electron microscopy

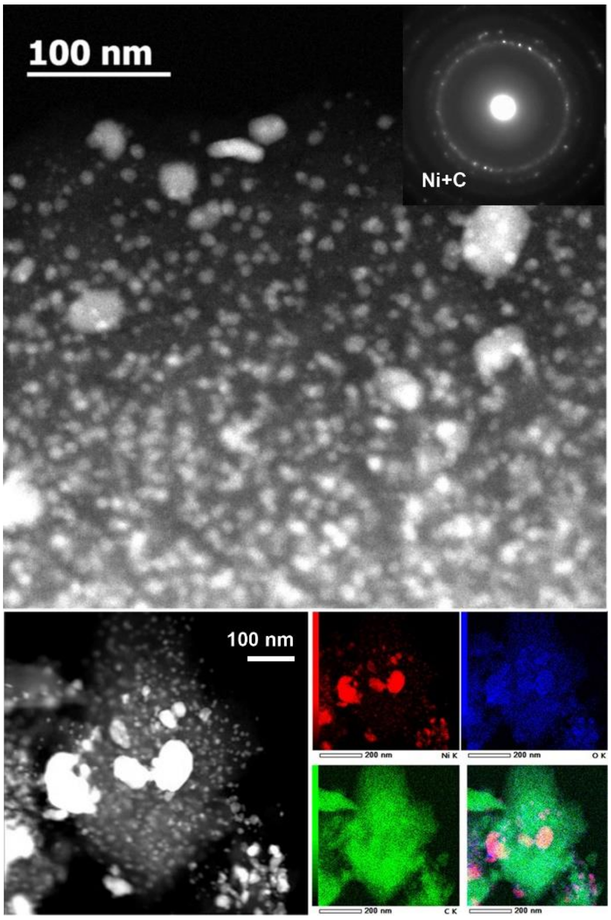

Fig. S10 HAADF−STEM images of Ni NPs in **as-synthesized Ni/AC–R** catalyst, together with elemental maps for Ni, O, C and their mixture. Inset in top panel is the corresponding ED pattern.

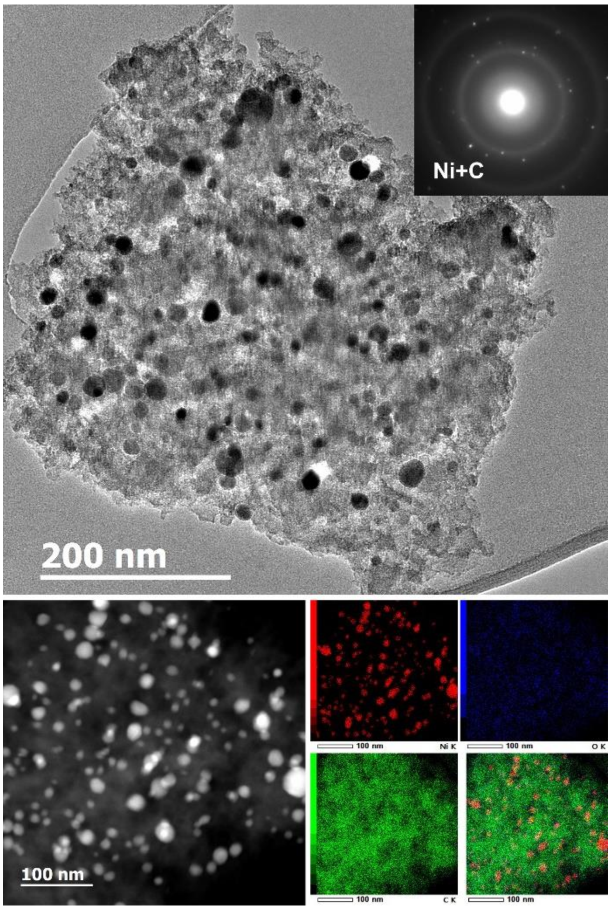

Fig. S11 TEM and HAADF–STEM images of Ni NPs in **spent Ni/AC–R** catalyst after 90 h on stream experiment, together with elemental maps for Ni, O, C and their mixture. Inset in top panel is the corresponding ED pattern.

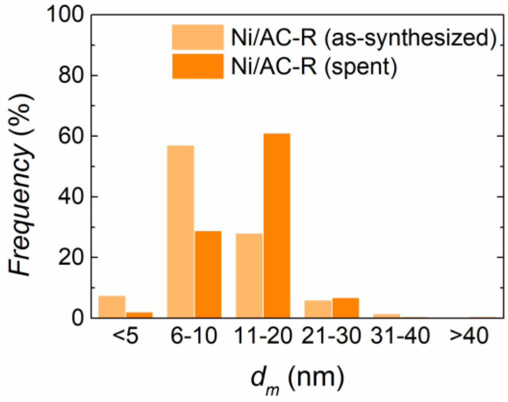

Fig. S12 Particle size distribution of the Ni NPs in **as-synthesized Ni/AC-R** and the same catalyst after the long time on stream experiment (90 h), calculated using the TEM images (**spent Ni/AC-R**).

X-ray photoelectron spectroscopy

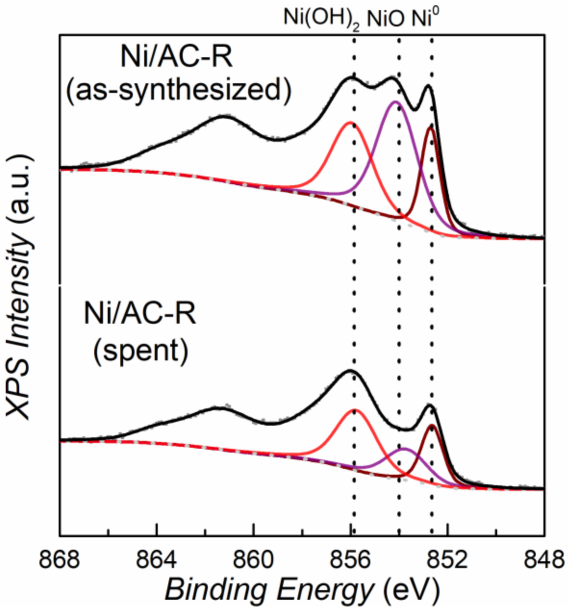

Fig. S13 High-resolution XPS data for Ni 2p$_{3/2}$ region of as-synthesized **Ni/AC-R** and the same catalyst after the long time on stream reaction experiment (90 h) (**Ni/AC-R spent**).

Table S4. Relative atomic percentage (at%) of Ni^0, NiO and Ni(OH)$_2$ phases in as-synthesized Ni/AC-R and the same catalyst after the long time on stream experiment (90 h) (spent Ni/AC-R), as estimated by XPS analysis.

Sample	*Ni^0 (relative at%)*	*NiO (relative at%)*	*Ni(OH)$_2$ (relative at%)*
Ni/AC–R (as-synthesized)	12	48	33
Ni/AC–R (spent)	26	26	49